Journal of Biotechnology 272–273 (2018) 22–32

Contents lists available at ScienceDirect

Journal of Biotechnology

journal homepage: www.elsevier.com/locate/jbiotec

Sensitive and specific detection of ligands using engineered riboswitches

Daniel P. Morse[a,*], Colin E. Nevins[a,1], Joana Aggrey-Fynn[b,2], Rick J. Bravo[a], Herman O.I. Pfaeffle[a,3], Jess E. Laney[a,4]

[a] Department of Chemistry, United States Naval Academy, Annapolis, MD 21402, USA
[b] Department of Biochemistry, Cell, and Molecular Biology, University of Ghana, Accra, Ghana

ARTICLE INFO

Keywords:
Riboswitch
Biosensor
Specificity
Sensitivity
In vitro
Selection

ABSTRACT

Riboswitches are RNA elements found in non-coding regions of messenger RNAs that regulate gene expression through a ligand-triggered conformational change. Riboswitches typically bind tightly and specifically to their ligands, so they have the potential to serve as highly effective sensors *in vitro*. In *B. subtilis* and other gram-positive bacteria, purine nucleotide synthesis is regulated by riboswitches that bind to guanine. We modified the *xpt-pbuX* guanine riboswitch for use in a fluorescence quenching assay that allowed us to specifically detect and quantify guanine *in vitro*. Using this assay, we reproducibly detected as little as 5 nM guanine. We then produced sensors for 2′-deoxyguanosine and cyclic diguanylate (c-diGMP) by appending the P1 stem of the guanine riboswitch to the ligand-binding domains of a 2′-deoxyguanosine riboswitch and a c-diGMP riboswitch. These hybrid sensors could detect 15 nM 2′-deoxyguanosine and 3 nM c-diGMP, respectively. Each sensor retained the ligand specificity of its corresponding natural riboswitch. In order to extend the utility of our approach, we developed a strategy for the *in vitro* selection of sensors with novel ligand specificity. Here we report a proof-of-principle experiment that demonstrated the feasibility of our selection strategy.

1. Introduction

Riboswitches are regulatory elements, found in the non-coding regions of messenger RNAs, that control gene expression through the direct sensing of signaling molecules (Serganov and Nudler, 2013). Binding of a specific ligand to a riboswitch stabilizes one of two alternative conformations resulting in either an increase ("ON" switch) or decrease ("OFF" switch) in the level of gene expression. Riboswitches can control transcription, translation, splicing, or RNA stability. To date, riboswitches have been discovered that respond to ions, purines and purine derivatives, enzyme cofactors, and amino acids. Since the discovery of riboswitches, there has been an explosion of interest in exploiting their high affinity and specificity for their ligands to develop biosensors for monitoring the concentration of compounds in living cells or in solution (Fowler et al., 2010; Fowler et al., 2013; You et al., 2015; Su et al., 2016). There is also great interest in using riboswitches as novel gene regulatory modules in synthetic biology (Topp and Gallivan, 2010; Chappell et al., 2013; Groher and Suess, 2014; Etzel and Morl, 2017; Hallberg et al., 2017).

Riboswitches are modular. They consist of a ligand-binding domain ("aptamer domain") and an "expression platform" that changes conformation in response to ligand binding. Sometimes, domains from two different riboswitches can be swapped to generate new synthetic riboswitches (Ceres et al., 2013aa,b; Litke et al., 2016; Rossmanith and Narberhaus, 2016). In addition, aptamers produced by *in vitro* selection have been successfully coupled to expression platforms to produce artificial riboswitches (also called "signaling aptamers") or to ribozymes to produce ligand-regulated allosteric "aptazymes" (Soukup and Breaker, 1999; Robertson and Ellington, 2000; Sharma et al., 2008). These constructs have been used to monitor ligand concentration *in vivo* and *in vitro* or to regulate gene expression in response to novel ligands.

We would like to produce new riboswitches with altered ligand specificity for use as biosensors. Producing highly effective biosensors through rational design is a challenging problem. Two examples from the literature are particularly relevant to our work. The purpose of these two experiments was not to produce effective sensors but to reveal the key elements that determine ligand specificity. Nonetheless, they illustrate the difficulty of using a rational design approach to

* Corresponding author.
E-mail address: morse@usna.edu (D.P. Morse).
[1] Present address: Bone and Joint Sports Medicine Institute, Naval Medical Center Portsmouth, 620 John Paul Jones Circle, Portsmouth, VA 23708, USA.
[2] Present address: Department of Molecular Biology and Genetics, Izmir Institute of Technology, Gulbahce Campus, Postal Code 35430, Urla, Izmir, Turkey.
[3] Present address: University of Virginia School of Medicine, Charlottesville, VA 22908, USA.
[4] Present address: McGovern Medical School at The University of Texas Health Science Center at Houston, 6431 Fannin, Houston, TX 77030, USA.

https://doi.org/10.1016/j.jbiotec.2018.03.002
Received 16 September 2017; Received in revised form 2 March 2018; Accepted 3 March 2018
Available online 05 March 2018
0168-1656/ Published by Elsevier B.V.

engineer biosensors with novel ligand specificity. C74 in the aptamer domain of the guanine riboswitch forms a Watson-Crick base pair with the guanine ligand (Serganov et al., 2004). When Gilbert et al. changed this C to U, the ligand preference changed from guanine to adenine but the mutant aptamer domain bound to adenine poorly compared to naturally-occurring adenine riboswitches (Gilbert et al., 2006). Adenine riboswitches have a U at position 74, but their sequences differ from that of the guanine riboswitch at many additional sites (Serganov et al., 2004). All of these differences are required to make them effective adenine sensors. Edwards and Batey gradually replaced sequences in the aptamer domain of the *xpt-pbuX* guanine riboswitch with the corresponding sequences from a 2′-deoxyguanosine riboswitch (Edwards and Batey, 2009). Only after extensive substitutions was a hybrid aptamer domain produced that could bind to 2′-deoxyguanosine with an affinity and specificity similar to the natural 2′-deoxyguanosine riboswitch.

Given the difficulties associated with rational design, it would be very useful to have a simple *in vitro* selection strategy for isolating riboswitches with novel ligand specificity. Traditional aptamers produced by *in vitro* selection are selected only for their ability to bind to a specific ligand. Thus, to produce an effective sensor by coupling a selected aptamer to an expression platform or to a ribozyme often requires extensive re-engineering and optimization (Ceres et al., 2013a,b; Soukup and Breaker, 1999; Robertson and Ellington, 2000). We and others have reported *in vitro* selection systems that directly select “signaling” aptamers that not only bind to a ligand but also signal the presence of the ligand by undergoing a specific conformational change (Nutiu and Li, 2005; Morse, 2007; Rajendran and Ellington, 2008; Vandenengel and Morse, 2009). Here we exploited the modular nature of naturally-occurring riboswitches to produce highly sensitive and specific sensors. We then used our sensor design and our previous approach for producing signaling aptamers as the bases for a selection strategy with the potential to directly select signaling aptamers with novel ligand specificity. We report a proof-of-principle experiment demonstrating the feasibility of our selection strategy.

2. Materials and methods

2.1. Fluorescence measurements

All measurements of fluorescence intensity were performed with a Modulus fluorometer (Turner Biosystems) in raw fluorescence mode using the blue fluorescence optical kit. Measurements were reported in “fluorescence standard units (FSU)”.

2.2. Oligonucleotides

Oligonucleotides were obtained from Integrated DNA Technologies, Inc. (IDT).

DM024 (GGTATAATAGGAACACTCATataatCGCGTGGATATGGCACGCAagtttctaccGGGCACCGTAAATGTCCgactATGGGTGAGCAATGGA). Encodes nucleotides 1–91 of the *xpt-pbuX* guanine riboswitch from *Bacillus subtilis* (Mandal et al., 2003). The first 2 nucleotides were changed from A to G for efficient transcription initiation by T7 RNA polymerase. The resulting RNA was called *xpt* RNA (1–91). For *in vitro* selection, the lower case bases were partially randomized.

JL001 (GGTATAATAGGAACACTCATAcagggtagcataatgggctactgacccgccttcaaacctatttggagacTATGGGTGAGCAATGGA). Encodes deoxyguanosine-guanine hybrid riboswitch. Upper case bases are from DM024. Lower case bases are from the 2′-deoxyguanosine riboswitch found in the ribonucleotide reductase gene of *Mesoplasma florum* (Kim et al., 2007).

DM025 (**GATAATACGACTCACTATA**GGTATAATAGGAACACTCA). Upstream primer for amplifying DM024 and JL001. Includes T7 promoter (bold) for *in vitro* transcription with T7 RNA polymerase.

DM026 (TCCATTGCTCACCCA). Downstream primer for amplifying DM024 and JL001 and for reverse transcription. This oligo was HPLC purified to guarantee that the 5′ end the oligo (3′ end of transcript) was intact.

JL002 (GGTATAATAGGAACACTCgcacagggcaaaccattcgaaagagtgggacgcaaagcctccggcctaaaccagaagacatggtaggtagcggggttaccGGGTGAGCAATGGA). Encodes c-diGMP-guanine hybrid riboswitch. Upper case bases are from the DM024. Lower case bases are from a c-diGMP riboswitch found in *Vibrio cholera* (Vc2) (Sudarsan et al., 2008). We removed one nucleotide from each of the priming sites so we used two new primers for PCR (DM025S and DM026S below).

DM025S (GATAATACGACTCACTATAGGTATAATAGGAACACTC). Upstream primer for amplifying JL002. It is identical to DM025 but is one nucleotide shorter.

DM026S (TCCATTGCTCACCC). Downstream primer for amplifying JL002. It is identical to DM026 but is one nucleotide shorter. This oligo was HPLC purified.

5′T-1(AGCATTGCTTGCTC). Corresponds to the sequence of the 5′ half of the terminator from the *xpt-pbuX* guanine riboswitch (Serganov et al., 2004).

3′T-1 (GAGCGGGCAATGCT). Corresponds to the sequence of the 3′ half of the terminator from the *xpt-pbuX* guanine riboswitch (Serganov et al., 2004).

5′T-7 labeled with quencher (5IAbFQ-CATTGCTCACCC). Variant of 5′T-1 chosen for use in fluorescence quenching assay. 5IAbFQ is the Iowa Black fluorescence quencher attached to the 5′ end.

5′T-7 labeled with biotin (5BiotinTEG-CATTGCTCACCC). Biotin is attached to the 5′ end of 5′T-7 *via* a 16 atom linker.

3′T-3 (GAGTGAGCAATG). Variant of 3′T-1 chosen for use in the fluorescence quenching assay.

Sequences of other oligonucleotides tested for use in the fluorescence quenching assay are given in Fig. 3.

2.3. Synthesis, labeling, purification, and quantification of RNA

Transcription templates were prepared by amplifying DM024, JL001, or JL002. Primers for amplifying DM024 and JL001 were DM025 and DM026. Primers for amplifying JL002 were DM025S and DM026S. Reaction contained: 5 μL (5 ng) oligonucleotide; 12 μL (240 pmol) of each primer; and 200 μL PCR supermix (Invitrogen). Reactions were divided into 4 equal aliquots and PCR was performed for 25 cycles. Each cycle consisted of 94 °C for 30 s, 45 °C for 30 s, and 72 °C for 30 s. PCR products were pooled, diluted to 400 μL with water, extracted once with phenol:chloroform:isoamyl alcohol (25:24:1 v/v), ethanol precipitated, and dissolved in 30 μL water. The upstream PCR primers (DM025 and DM025S) included a T7 RNA polymerase promoter at their 5′ ends allowing the PCR products to be used as templates for *in vitro* transcription. *In vitro* transcription was performed with the TranscriptAid T7 High Yield Transcription Kit (Thermo Scientific). Reactions contained: 30 μL (~600 ng) PCR product; 85 μL water; 64 μL 5× buffer; 116 μL 25 mM NTPs; 25 μL enzyme soln. Reactions were split into 2 equal aliquots and incubated for 6 h at 40 °C. 2 μL of 1 U/μL DNase was added to each tube and incubation was continued for another 15 min. After incubation, precipitates formed (likely pyrophosphate). The precipitates were pelleted by spinning for 3 min at top speed in a microcentrifuge, and the supernatants were transferred to new tubes. The samples were extracted twice with phenol:chloroform:isoamyl alcohol (25:24:1 v/v). Each reaction was split into 4 equal aliquots. Each aliquot was diluted to 400 μL with water and the RNA was precipitated. Each pellet was dissolved in 100 μL of water and two aliquots of 50 μL were each passed through a chromaspin-10 gel filtration spin column (Clontech). Each aliquot was diluted to 400 μL with water and precipitated and the pellets were dissolved in 100 μL of water. The aliquots were combined and the concentration of the RNA was determined by absorbance at 260 nm. Each RNA was labeled by oxidizing the 3′ ends with sodium periodate (Sigma) and reacting the oxidized RNA with fluorescein-5-thiosemicarbazide (Sigma). Oxidation reactions contained: 144 μL (150 μg) RNA; 18 μL 200 mM $NaCH_3COO$

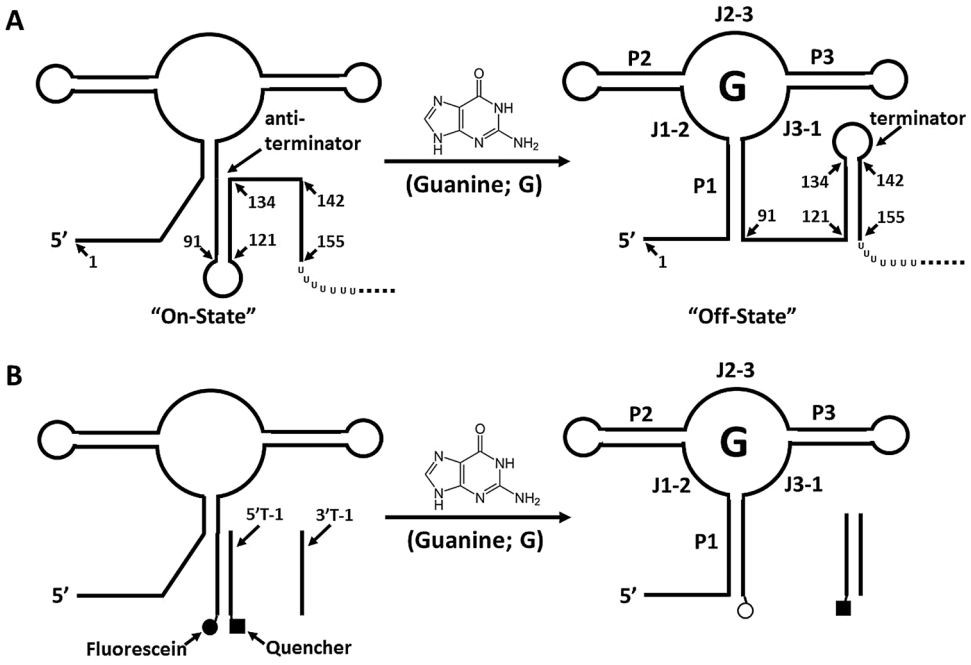

Fig. 1. (A) *In vivo* regulation of gene expression by the *xpt-pbuX* guanine riboswitch. The diagram represents nucleotides 1–161 of the *xpt-pbuX* mRNA. Upon binding to guanine, a conformational change disrupts the antiterminator and a premature terminator forms when nucleotides 121–134 pair with nucleotides 142–155. P1, P2, and P3 are base-paired regions in the guanine-bound form of the riboswitch. J1-2, J2-3, and J3-1 are joining regions. The dotted line indicates that the mRNA continues in the 5' to 3' direction. **(B)** Diagram showing how the riboswitch was adapted for use as a guanine sensor *in vitro*. RNA corresponding to nucleotides 1–91 of the *xpt-pbuX* mRNA was synthesized by in vitro transcription. 5'T-1 and 3'T-1 are synthetic DNA oligonucleotides with sequences corresponding to nucleotides 121–134 and 142–155, respectively, in the natural riboswitch. The riboswitch RNA was labeled at its 3' end with fluorescein. 5'T-1 was labeled at its 5' end with a quencher. Binding of guanine would produce an increase in the fluorescence intensity (indicated by fluorescein changing from filled to open circle) if the quencher moves away from the fluorescein. (The sequences of 5'T-1 and 3'T-1 had to be changed to produce a functional sensor).

pH 5.5; and 18 µL 200 mM $NaIO_4$ (0.5 g/10 mL; made fresh). The reactions were incubated for 1 h at room temperature in the dark. Excess $NaIO_4$ was consumed by adding 180 µL of 2% ethylene glycol and incubating for 10 min at room temperature in the dark. Each reaction was diluted to 800 µL with water, divided into two aliquots of 400 µL and the RNA was precipitated. The pellets were dissolved in 400 µL of water and the RNA was precipitated again and each pellet was dissolved in 97.5 µL of water and combined. Labeling reactions contained 195 µL of RNA from the oxidation reactions; 22.5 µL 1 M $NaCH_3COO$ pH 5.5; 7.5 µL 100 mM fluorescein-5-thiosemicarbazide dissolved in dimethylformamide (Sigma). Reactions were incubated for 1 h at room temperature in the dark. The reactions were diluted to 400 µL with water and precipitated. Both labeled and unlabeled RNAs were purified from an 8% polyacrylamide gel by electroelution using D-tube dialysis tubes (Novagen). Electroeluted RNAs were precipitated and dissolved in 100 µL water. The concentration of each RNA was determined by absorbance at 260 nm. An aliquot of each labeled and gel-purified RNA was diluted 200-fold and the fluorescence intensity was measured. Fluorescence intensity was typically about 1.5×10^5 FSU per pmol of RNA.

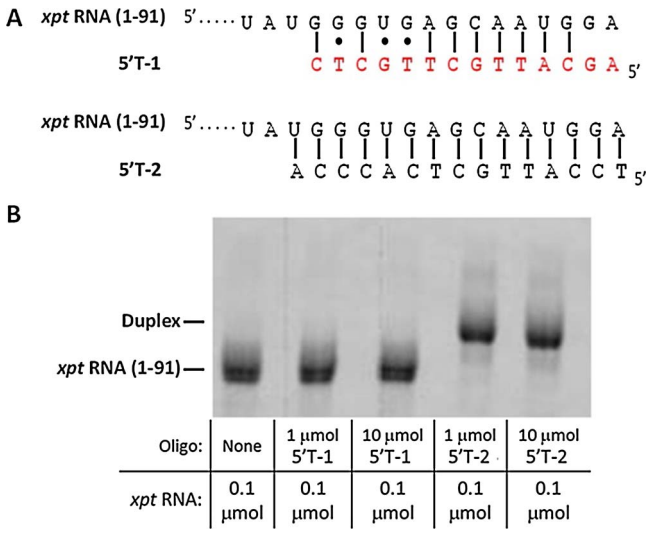

Fig. 2. 5'T-1 does not form a stable duplex with *xpt* RNA (1–91). **(A)** Figure illustrating base-pairing between *xpt* RNA (1–91) and the DNA oligonucleotides 5'T-1 (top) or 5'T-2 (bottom). 5'T-1 corresponds to nucleotides 121-134 of the guanine riboswitch. It was expected to form an imperfect 12 bp duplex with *xpt* RNA (1–91). 5'T-2 was a positive control that formed a perfect 15 bp duplex with *xpt* RNA (1–91). Solid lines represent Watson-Crick base pairs. Dots represent non-Watson-Crick base pairs. **(B)** Electrophoretic mobility shift assay (EMSA) of duplex formation. The positions of *xpt* RNA (1–91) and the duplex formed with 5'T-2 are indicated on the left side of the non-denaturing gel. Under our assay conditions, 5'T-1 did not form a stable duplex with *xpt* RNA (1–91) even when present at a 100-fold molar excess. 5'T-2 formed a stable duplex with *xpt* RNA (1–91) when present at a 10-fold molar excess. [Duplex formation went to completion with a 1:1 molar ratio of *xpt* RNA (1–91) and 5'T-2; not shown].

2.4. Electrophoretic mobility shift assays (EMSA)

To identify DNA oligonucleotides that could efficiently form a stable duplex with *xpt* RNA (1–91), we purchased 9 oligonucleotides (5′T-2 through 5′T-10) predicted to have a range of melting temperatures (T_m) when annealed to *xpt* RNA (1–91). 10 µL annealing reactions contained 0.1 µmol of fluorescein-labeled RNA, 0, 0.1, 1, or 10 µmol of oligonucleotide, and assay buffer (100 mM KCl, 50 mM Tris-HCl, pH 7.4). The mixtures were heated at 65 °C for 3 min and cooled to room temperature. To separate duplexes from single stranded nucleic acids, each annealing reaction was run on an 8% non-denaturing polyacrylamide gel at room temperature. The RNA-DNA duplexes and single-stranded RNAs were visualized on a UV trans-illuminator.

To identify DNA oligonucleotides that could efficiently compete with *xpt* RNA (1–91) for pairing with 5′T-7 in the presence of guanine, we purchased 5 oligonucleotides (3′T-2 through 3′T-6) predicted to have a range of melting temperatures when annealed to 5′T-7 and performed strand-exchange reactions. After preparing 10 pmol of the *xpt* RNA (1–91)/5′T-7 duplex as described above, 20 pmol of competing oligonucleotide in assay buffer, and 0, 20, or 40 pmol of guanine in assay buffer were added to a total volume of 15 µL. The reaction products were separated and visualized as describe above for the annealing reaction. A successful strand-exchange reaction resulted in the release of single-stranded *xpt* RNA (1–91) from the *xpt* RNA (1–91)/5′T-7 duplex. After testing a variety of reaction temperatures and incubation times, we found that incubating the reaction overnight (~18 h) at 4 °C gave the best signal-to-background ratio.

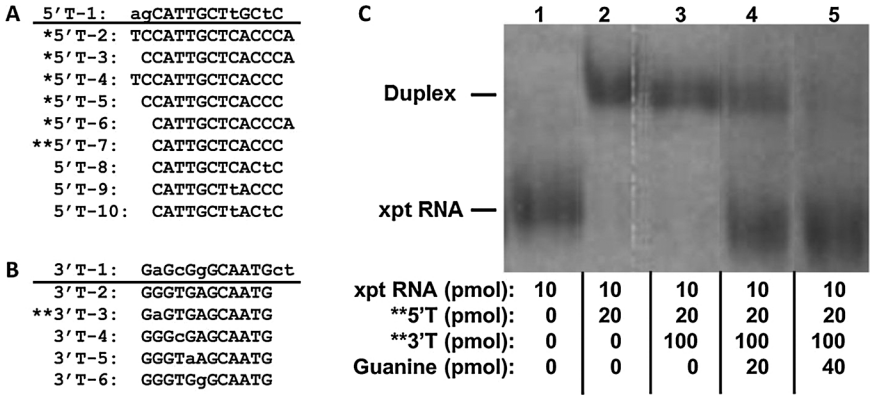

Fig. 3. Identifying DNA oligonucleotides that function efficiently in the strand-exchange reaction. **(A)** Oligonucleotides tested for their ability to form a stable duplex with *xpt* RNA (1–91). The sequence of 5′T-1 is the same as the 5′ half of the terminator in the ligand-bound form of the guanine riboswitch. Bases that are not complementary to *xpt* RNA (1–91) are in lower case. Asterisks indicate oligos that could form a stable duplex with *xpt* RNA (1–91) when present in stoichiometric amounts. 5′T-7 (indicated by **) was chosen for use in the strand-exchange reaction. **(B)** Oligonucleotides tested for their ability to compete with *xpt* RNA (1–91) for pairing with 5′T-7. The sequence of 3′T-1 is the same as the 3′ half of the terminator in the ligand-bound form of the guanine riboswitch. Bases that are not complementary to 5′T-7 are in lower case. 3′T-3 (indicated by **) was chosen for use in the strand-exchange reaction. **(C)** Strand-exchange reaction. The positions of fluorescein-labeled xpt RNA (1–91) (lane 1) and the duplex formed with 5′T-7 are indicated on the left side of the non-denaturing gel. When strand-exchange occurred, the duplex was converted into free *xpt* RNA (1–91). Very little strand-exchange occurred in the absence of guanine and 3′T (lanes 2) or in the presence of 3′T alone (lane 3). Strand-exchange occurred in the presence of 3′T plus 20 pmol of guanine (lane 4) and neared completion in the presence of 3′T and 40 pmol of guanine (lane 5).

2.5. Fluorescence quenching assay

The following ligands were purchased from Sigma: guanine, adenine, hypoxanthine, guanosine, 2′-deoxyguanosine, 3′-deoxyadenosine, 2′-guanosine monophosphate (2′-GMP), 3′-guanosine monophosphate (3′-GMP), 3′,5′-cyclic diguanylate (c-diGMP), 3′,5′-cyclic diadenylate (c-diAMP), and 2′,5′-3′,5′-cyclic guanosine monophosphate-adenosine monophosphate (c-GAMP). Reactions (70 µL total volume) contained: 25 pmol unlabeled riboswitch RNA; 10 pmol riboswitch RNA labeled at its 3′ end with fluorescein; 70 pmol 5′T-7 with quencher at its 5′ end; 350 pmol 3′T-3; assay buffer; and a variable concentration of ligand as indicated in the figures. Reactions with the 2′-deoxyguanosine-guanine hybrid and the c-diGMP-guanine hybrid riboswitches also included 2 mM $MgCl_2$. Prior to adding 3′T-3 and the ligand, 5′T-7 was annealed to the riboswitch RNA by heating at 65 °C for 3 min in assay buffer and cooling to room temperature. The annealing reaction and a mix containing 3′T-3, ligand, and assay buffer (including $MgCl_2$ when needed) were placed on ice. After 5 min on ice, the mix was added to the annealing reaction and incubated at 4 °C for ~18 h. After incubation, the fluorescence intensity was measured at 4 °C using assay buffer as the blank. A one-tailed *T*-test assuming equal variance was used to determine if signals were greater than background.

2.6. Preparation of initial partially randomized RNA pool for selection

An oligonucleotide pool containing a large number of variants of the guanine riboswitch was synthesized by IDT (see oligonucleotide DM024 in Section 2.2). Each of the lower case bases shown in the DM024 sequence was 27% randomized. For example, consider a randomized position that is shown as an A in DM024. Of the oligonucleotides in the

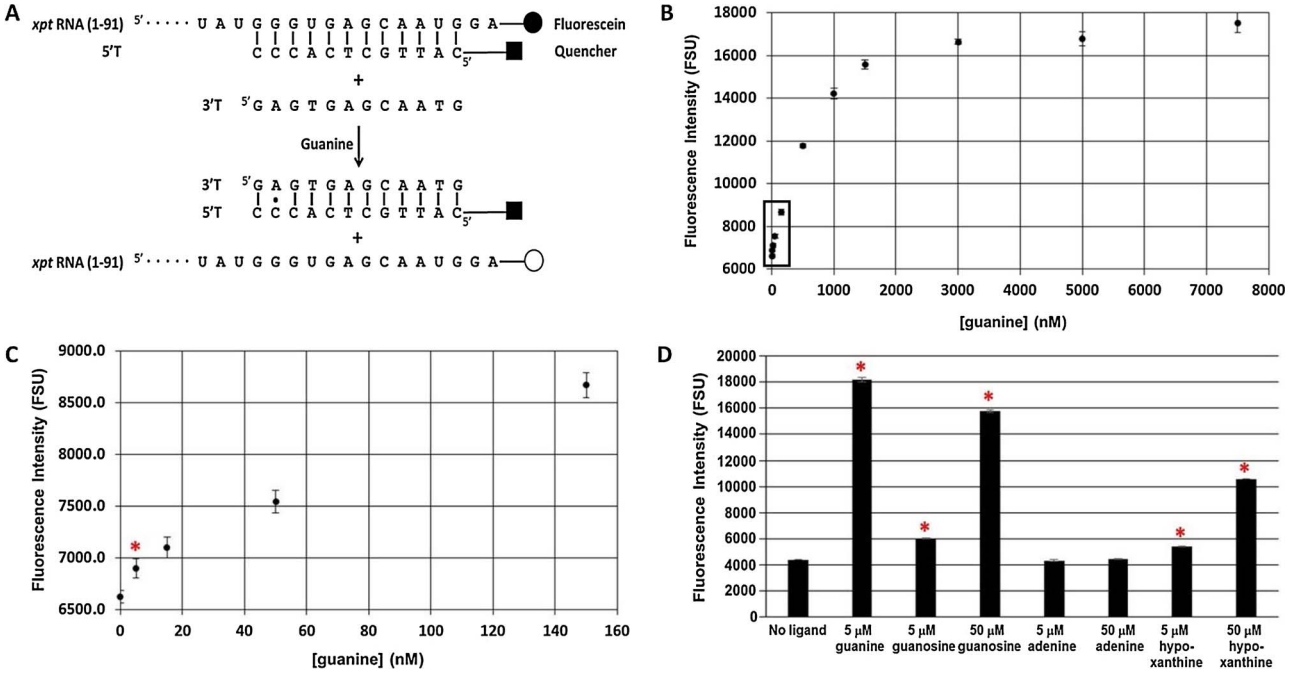

Fig. 4. The fluorescence quenching assay for guanine. **(A)** Assay design. 5′T-7 and 3′T-3 are DNA oligonucleotides chosen for the assay after screening a number of oligo pairs. When guanine binds to *xpt* RNA (1–91), 5′T-7 dissociates form the RNA and pairs with 3′T-3 producing an increase in fluorescence intensity as the quencher moves away from the fluorophore. **(B)** Fluorescence intensity as a function of guanine concentration. The sensor was saturated at ~3 µM guanine. **(C)** Enlargement of the boxed region of the graph in (B) showing that the sensor can reproducibly detect as little as 5 nM guanine. Fluorescence values are the averages of 4 independent reactions. Error bars are standard deviations. The asterisk indicates that the signal at 5 nM guanine is significantly higher than background ($P = 3 \times 10^{-4}$). **(D)** The guanine sensor retains the ligand specificity of the natural guanine riboswitch. The signal produced by 5 µM guanine was compared to that produced by 5 µM and 50 µM guanosine, adenine, or hypoxanthine. Asterisks indicate signals that were significantly greater than background ($P < 0.05$).

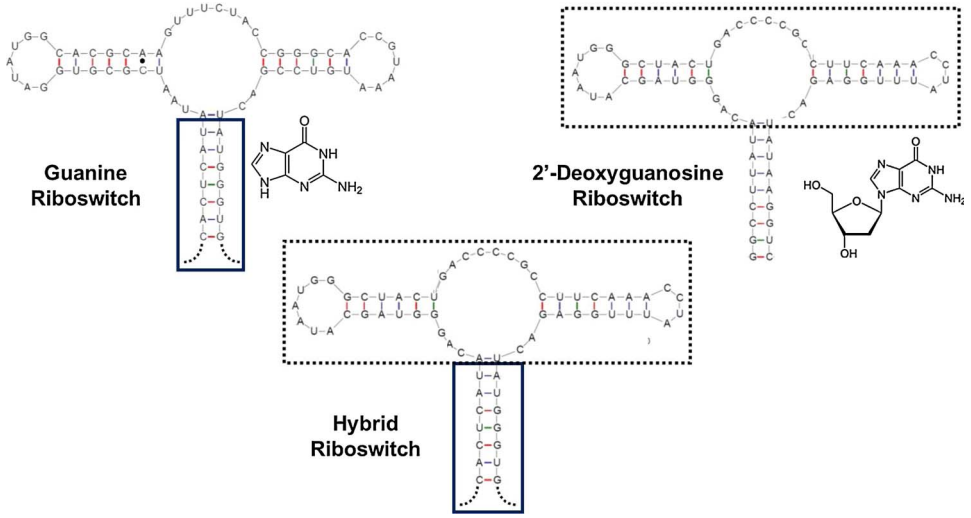

Fig. 5. Predicted secondary structures of the guanine, 2'-deoxyguanosine, and hybrid riboswitches. The solid box indicates the P1 stem and flanking nucleotides 1–13 and 82–91 (dotted lines) of the guanine riboswitch. The dotted box indicates the ligand-binding domain of the 2'-deoxyguanosine riboswitch. The structures of guanine and 2'-deoxyguanosine are shown.

randomized pool, 73% have an A, 9% have a G, 9% have a C, and 9% have a T at this position. The transcription template was made by amplifying the randomized oligonucleotide pool using DM025 and DM026 as primers. A total of 40 pmol ($\sim 2 \times 10^{13}$ molecules) of the randomized oligonucleotide pool was amplified in 30 independent reactions (50 µL each). The randomized RNA pool was synthesized, labeled, purified, and quantified as described above.

2.7. In vitro selection procedure

The selection strategy is illustrated in Fig. 9A. 200 pmol of biotinylated 5′T-7 was attached to 2 mg of streptavidin-coated magnetic beads (Dynabeads M-270 streptavidin from Invitrogen) according to manufacturer's instructions. The beads were captured with a magnetic stand (Promega) and the liquid was removed. 180 pmol of fluorescein-labeled randomized RNA in 200 µL of hybridization buffer (50 mM Tris pH 7.4, 500 mM NaCl) was added to the beads and the mixture was rotated overnight at 25 °C to allow the RNA to anneal to immobilized 5′T-7. After RNA binding, unbound RNA was removed as follows: beads were rinsed 4 times quickly at 25 °C, twice for 30 min at 25 °C, and once for 30 min at 4 °C with 400 µL of assay buffer. The mixture was continuously rotated during each 30 min incubation. Beads were captured between each rinse and the liquid was discarded. Bound RNA was eluted for various times by rotating at 4 °C in 200 µL assay buffer

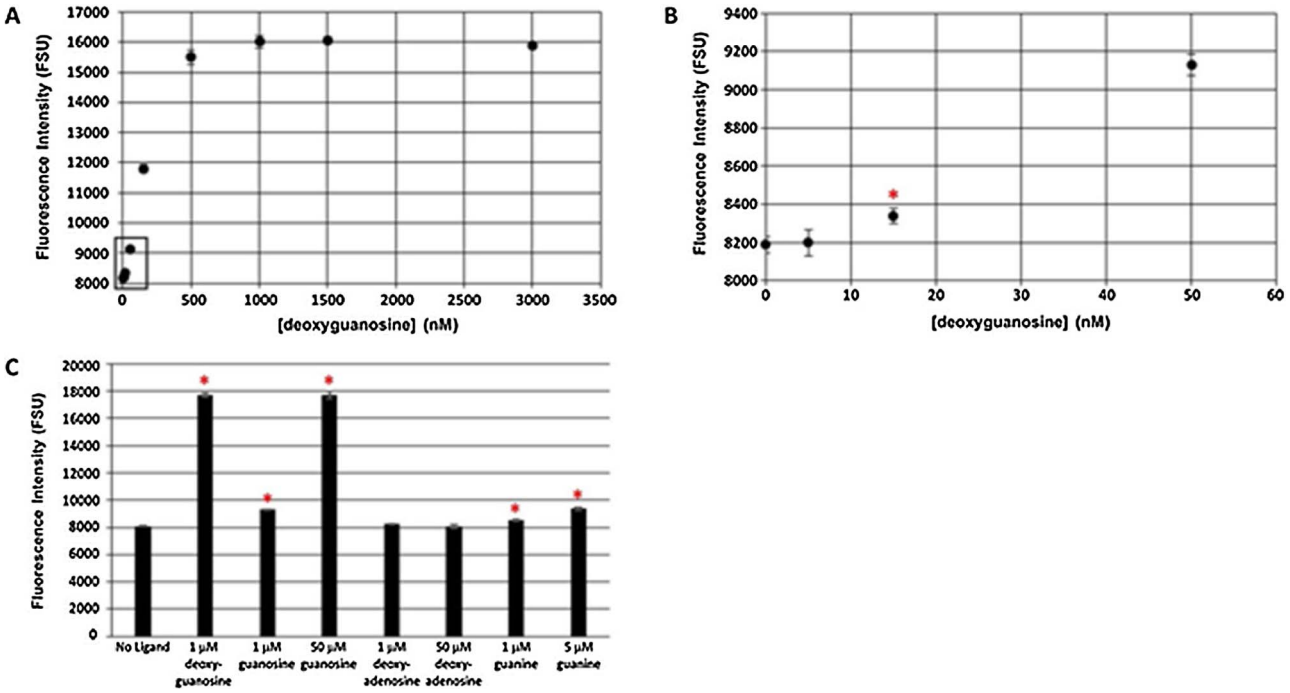

Fig. 6. Sensitivity and specificity of the 2'-deoxyguanosine hybrid sensor. **(A)** Fluorescence intensity as a function of 2'-deoxyguanosine concentration. The sensor was saturated at ~1 µM 2'-deoxyguanosine. **(B)** Enlargement of the boxed region of the graph in (A) showing that the sensor can reproducibly detect as little as 15 nM 2'-deoxyguanosine. Fluorescence values are the averages of 3 independent reactions. Error bars are standard deviations. The asterisk indicates that the signal at 15 nM 2'-deoxyguanosine is significantly higher than background ($P = 0.005$). **(C)** The sensor retains the specificity of the natural 2'-deoxyguanosine riboswitch. The signal produced by 1 µM 2'-deoxyguanosine was compared to that produced by 1 µM and 50 µM guanosine, 1 µM and 50 µM 2'-deoxyadenosine, or 1 µM and 5 µM guanine. Fluorescence values are the averages of 3 independent reactions. Error bars are standard deviations. Asterisks indicate signals that were significantly higher than background ($P < 0.05$).

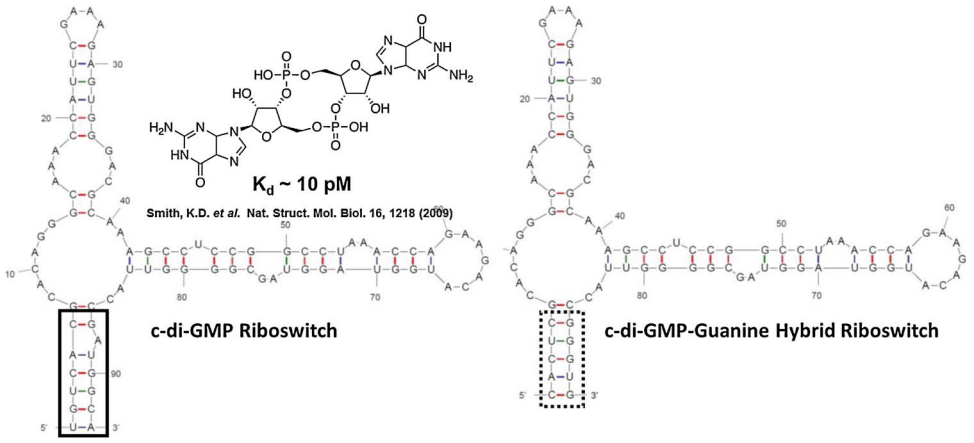

Fig. 7. Predicted secondary structures of the c-diGMP riboswitch and the hybrid riboswitch. The solid box indicates the region of the c-diGMP riboswitch that was replaced with a truncated version of the P1 stem from the guanine riboswitch (dotted box). The top two base pairs of P1 were deleted in order to obtain the desired predicted secondary structure. The structure of c-diGMP is shown.

containing 5 µM guanine and the eluted RNA was collected. RNA that remained bound to the beads was removed by heating 3 times in 600 µL of hybridization buffer for 3 min at 55 °C. The RNA removed by each round of heating was collected in a single tube. The amount of RNA that eluted with ligand and the amount of RNA removed from the beads by heating was determined by measuring the fluorescence intensity of a small aliquot of each of the two fractions. The amount of RNA that bound to the 5′T-7 beads was calculated as the amount of RNA eluted with ligand plus the amount of RNA removed by heating. The elution efficiency was calculated as the percentage of bound RNA eluted with ligand. The level of background elution was determined in control experiments in which the RNA was eluted with assay buffer. We found that the highest signal-to-background ratio was achieved when the RNA was eluted for 6 h. The eluted RNA was precipitated and dissolved in 19.2 µL of water. The RNA was amplified by reverse transcription and PCR followed by transcription. Reverse transcription reactions contained: 19.2 µL RNA; 2 µL DM026 (50 pmol); 1.6 µL 10 mM dNTP; 6.4 µL 5× buffer (supplied with enzyme); 1.6 µL 100 mM DTT; and 1.2 µL (300 U) MLV reverse transcriptase (Invitrogen). The reactions were incubated for 1 h at 42 °C. PCRs contained: 32 µL cDNA (from reverse transcription); 16 µL (400 pmol) DM025; 16 µL (400 pmol) DM026; and 288 µL PCR supermix. Each reaction was divided into 6 equal aliquots and cycling was performed as described above. The PCR products were pooled, diluted to 400 µL with water, extracted once with phenol-chloroform-isoamyl alcohol (25:24:1 v/v), and precipitated. All of the PCR product was used for *in vitro* transcription. Transcription, labeling, and gel-purification were performed as described in the section above called “Synthesis, labeling, purification, and quantification of RNA”. The selection process was repeated until the percentage of bound RNA eluted with guanine reached a maximum.

2.8. Cloning and sequencing of cDNAs

PCR products made from selected RNA was cloned using a TA cloning kit (Invitrogen) according to the manufacturer’s instructions. Inserts were sequenced using the M13 reverse primer. Sequencing was performed by Eurofins Genomics. Sequence alignments were performed with Megalign which is part of the Lasergene software package from DNAStar.

3. Results

3.1. Adapting a guanine riboswitch for use as a guanine sensor in vitro

In vivo, guanine binding stabilizes a conformation of the guanine riboswitch that includes a premature transcriptional terminator (Fig. 1A). We attempted to convert the *xpt-pbuX* guanine riboswitch (Mandal et al., 2003) into a sensor by using 3 fragments of the riboswitch as shown in Fig. 1B. We synthesized the first 91 nucleotides of the riboswitch by *in vitro* transcription and labeled the RNA at its 3′ end with fluorescein. This fragment, which we called *xpt* RNA (1–91), spans the aptamer domain of the riboswitch. The other two fragments were DNA oligonucleotides, called 5′T-1 and 3′T-1, with sequences that corresponded to the 5′ and 3′ halves of the terminator stem. In addition to pairing with 3′T-1 to form an analog of the terminator, 5′T-1 can pair with the 3′ end of *xpt* RNA (1–91) to form a duplex that mimics the antiterminator (compare Fig. 1A and B). The strategy for our *in vitro* guanine assay was to label 5′T-1 at its 5′ end with a quencher, anneal it to fluorescein-labeled *xpt* RNA (1–91), and incubate the duplex with guanine and 3′T-1. We anticipated that guanine binding to *xpt* RNA (1–91) would stabilize the P1 stem resulting in a strand-exchange reaction in which 5′T-1 dissociates from *xpt* RNA (1–91) and anneals to 3′T-1 (Fig. 1B). Thus, we expected to observe an increase in the fluorescence intensity as the quencher moved away from the fluorescein. Recently, Steinert et al. used a similar system to study the kinetics of this strand-switching reaction (Steinert et al., 2017).

We first used an electrophoretic mobility shift assay (EMSA) to determine whether we could anneal 5′T-1 to *xpt* RNA (1–91) to form a structure analogous to the antiterminator. We chose to exclude magnesium ions from the reaction to prevent Mg^{2+}-catalyzed hydrolysis of the RNA during the annealing reaction. We found that 5′T-1 and *xpt* RNA (1–91) could not form a stable duplex at room temperature even when 5′T-1 was present in 100-fold molar excess (Fig. 2). As a positive control we performed the same experiment using an oligo (called 5′T-2) that could form a 15 base-pair perfect duplex with *xpt* RNA (1–91). This annealing reaction went to completion in the presence of a 10-fold or 100-fold molar excess of 5′T-2 (Fig. 2). In fact, the reaction with 5′T-2 went to completion even when added to *xpt* RNA (1–91) in a 1:1 ratio (data not shown). Since the desired duplex with 5′T-1 was unstable in the absence of magnesium ions, we needed to find an oligo that could form a stable, but not too stable, duplex with *xpt* RNA (1–91) under our chosen conditions. We reasoned that if the duplex was too stable, it would not efficiently undergo the desired strand-exchange reaction. Therefore, we used the EMSA to test a variety of oligos for their ability to anneal to *xpt* RNA (1–91). We identified 5 oligos that formed a stable duplex at room temperature in the absence of magnesium ions when mixed with *xpt* RNA (1–91) at a 1:1 M ratio (Fig. 3A). We chose oligonucleotide 5′T-7 for further study because it formed the duplex with the lowest predicted melting temperature.

The sequences of 5′T-1 and 3′T-1 were the same as that found in the natural guanine riboswitch. Since we could not use 5′T-1, we reasoned that we would have to find an alternative to 3′T-1. We used the EMSA to find oligonucleotides that could efficiently compete with *xpt* RNA (1–91) for pairing with 5′T-7 in the presence, but not in the absence, of guanine. Fig. 3B shows the sequences of the oligos tested. 3′T-3 was the oligo that worked best in this strand-exchange assay. We looked for

conditions that gave the highest "signal-to-background" ratio. That is, we wanted to minimize the amount of strand-exchange that occurred in the absence of guanine (the "background") and maximize the amount of strand-exchange that occurred in the presence of guanine (the "signal"). We found the optimal reaction conditions to be as follows: 1:2:10 ratio of *xpt* RNA (1–91) to 5′T-7 to 3′T-3 in 50 mM Tris pH 7.4 and100 mM KCl incubated overnight (~18 h) at 4 °C (Fig. 3C). Under these conditions, there was very little background (Fig. 3C, Lane 3) and, in the presence of a 4:1 ratio of guanine to *xpt* RNA (1–91), the strand-exchange reaction went nearly to completion (Fig. 3C, Lane 5). Importantly, inclusion of 2 mM $MgCl_2$ significantly decreased the signal-to-background ratio due to an increase in the background (data not shown).

Next, we performed the fluorescence-quenching assay. Fig. 4A shows the desired guanine-triggered strand exchange reaction. As expected, the fluorescence intensity increased with guanine concentration and reached a maximum at about 1 μM guanine (Fig. 4B). The assay was highly reproducible allowing us to detect as little as 5 nM guanine (Fig. 4C). To assess the ligand specificity of the assay, we compared the signal produced by 5 μM guanine to that produced by 5 μM or 50 μM guanosine, adenine, and hypoxanthine. As expected from previously reported dissociation constants for these ligands (Mandal et al., 2003; Gilbert et al., 2009), our sensor could detect guanosine and hypoxanthine but with reduced sensitivity compared to guanine, and could not detect 50 μM adenine (Fig. 4D).

3.2. Hybrid sensors for the detection of other ligands

We wanted to extend our approach to other riboswitches. However, we did not want to have to re-optimize the sequences of the DNA oligonucleotides and the assay conditions for each new sensor. Therefore, we asked whether we could use hybrid riboswitches composed of the P1 stem from the guanine riboswitch (and some flanking single-stranded RNA) and the ligand-binding domain of a different riboswitch. If so, we could produce sensors for a variety of ligands that allowed us to use the same oligonucleotides (5′T-7 and 3′T-3) and the same conditions as used for the guanine assay.

We attached the ligand-binding domain of a 2′-deoxyguanosine riboswitch from *M. florum* (Kim et al., 2007) to the P1 stem of the guanine riboswitch and performed fluorescence quenching assays. The design of the sensor is shown in Fig. 5. The results of the assays are shown in Fig. 6. We used the program M-fold (http://unafold.rna.albany.edu/?q=mfold/RNA-Folding-Form) to verify that our hybrid construct was likely to adopt the desired secondary structure in the absence of 5′T-7. We were able to use the same assay conditions as used in the guanine assay except we found that this reaction required the presence of magnesium ions. ($MgCl_2$ was added after annealing 5′T-7 to the hybrid sensor to avoid Mg^{2+}-catalyzed RNA hydrolysis at high temperature.) The signal with the hybrid sensor reached a maximum at about 1 μM 2′-deoxyguanosine (Fig. 6A). Although inclusion of 2 mM Mg^{2+} increased the background, the hybrid sensor was able to reproducibly detect as little as 15 nM 2′-deoxyguanosine (Fig. 6B). The sensor retained the same ligand specificity as the naturally-occurring 2′-deoxyguanosine riboswitch (Kim et al., 2007). In addition to 2′-deoxyguanosine, the sensor could detect guanosine and guanine but with much lower sensitivity (Fig. 6C). The sensor could not detect 50 μM 2′-deoxyadenosine.

Next, we attached the ligand-binding domain of a 3′,5′-cyclic-di-guanylate (c-diGMP) type I riboswitch from *V. cholerae* (Sudarsan et al., 2008) to a truncated version of the P1 stem of the guanine riboswitch. We found that we had to remove two base-pairs from near the top of the P1 stem in order for the hybrid sensor to fold into the proper secondary structure as predicted by the program M-fold. The design of the hybrid sensor is shown in Fig. 7. The results of the fluorescence-quenching assays are shown in Fig. 8. As with the 2′-deoxyguanosine sensor, the c-diGMP sensor worked only in the presence of magnesium ions. The maximum signal was obtained with ~3 μM c-diGMP (Fig. 8A) and we could reproducibly detect as little as 3 nM c-diGMP (Fig. 8B). Fig. 8C

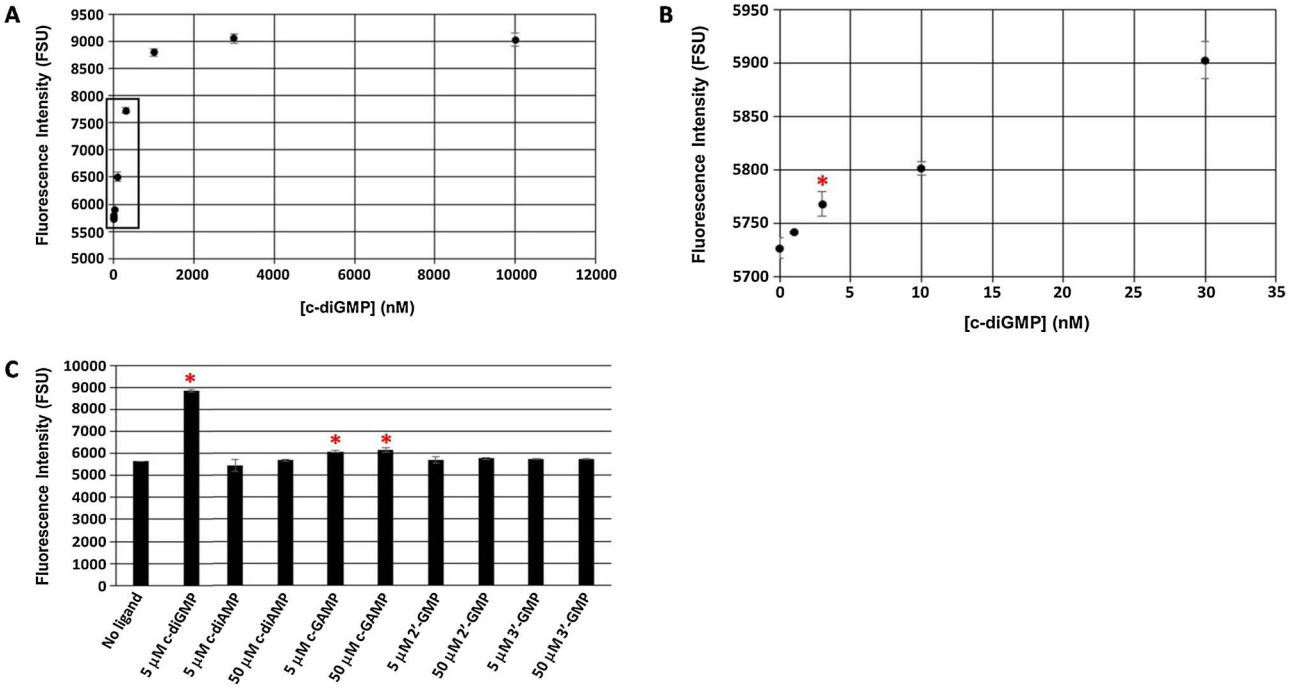

Fig. 8. Sensitivity and specificity of the 3',5'-c-diGMP hybrid sensor. **(A)** Fluorescence intensity as a function of c-diGMP concentration. The sensor was saturated at ~3 μM c-diGMP. **(B)** Enlargement of the boxed region of the graph in (A) showing that the sensor can reproducibly detect as little as 3 nM c-diGMP. Fluorescence values are the averages of 3 independent reactions. Error bars are standard deviations. The asterisk indicates that the signal at 3 nM c-diGMP is significantly higher than background ($P = 0.005$). **(C)** The sensor retains the specificity of the natural c-diGMP riboswitch. The signal produced by 5 μM 3,5'-c-diGMP was compared to that produced by 5 μM and 50 μM 3',5'-c-diAMP; 2',5'-3',5'-c-GAMP; 2'-GMP; or 3'-GMP. Fluorescence values are the averages of 3 independent reactions. Error bars are standard deviations. Asterisks indicate signals that are significantly higher than background ($P < 0.05$).

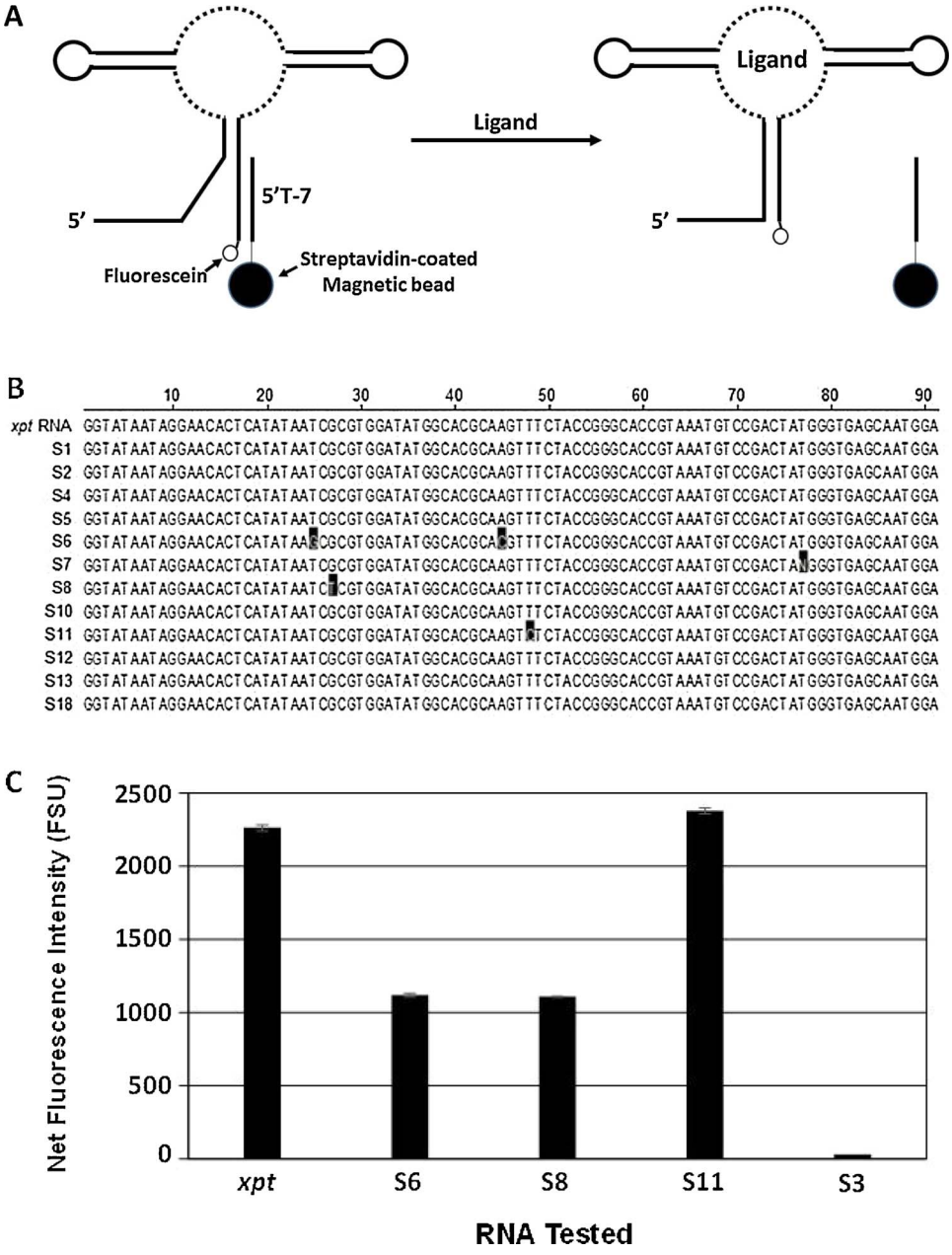

Fig. 9. (A) *In vitro* selection strategy for selecting riboswitch variants with novel ligand specificity. The system is identical to the quenching assay shown in Fig. 1B except the quencher on 5′T-7 was replaced with a magnetic bead via a biotin-streptavidin interaction, and the sequence of the ligand- binding domain (dotted line) was partially randomized. 3′T-3 is not shown because it was not included in the selection experiment discussed in the text. **(B)** Alignment of the *xpt* RNA (1–91) cDNA with cDNA sequences selected with guanine. Bases that differ from those found in *xpt* RNA (1–91) are highlighted in black. "N" represents a base that could not be called by the sequencing software which was assumed to be a "T". Nucleotides 21-75 were partially randomized. **(C)** Assay of selected RNA function. Using the fluorescence quenching assay, the ability of selected RNAs S6, S8, S11, or S3 to detect 100 nM guanine was compared to that of *xpt* RNA (1–81). The y-axis (Net Fluorescence Intensity) is the difference between the fluorescence intensity produced in the presence of 100 nM guanine minus the background fluorescence produced in the absence of ligand. Values are the averages of 3 independent reactions. Error bars are standard deviations. Unlike S6, S8, and S11 RNAs, the fluorescence intensity produced by S3 RNA was not significantly higher than background.

shows that the sensor is highly specific for c-diGMP. It could not detect 50 μM 3′,5′-c-diAMP, 2′-GMP, or 3′-GMP. The signal produced by c-GAMP (2′,5′-3′,5′-cyclic guanosine monophosphate-adenosine monophosphate) at 1 μM was barely above background. Surprisingly, the signal did not increase with 50 μM c-GAMP. One possible explanation is that c-GAMP binds readily to the sensor but only poorly induces the strand-exchange reaction.

3.3. Strategy for the selection of sensors with novel ligand specificity: proof-of-principle

To further extend the utility of our approach, we devised an *in vitro* selection scheme to produce sensors with novel ligand specificity. The idea is to partially randomize the sequence of an existing sensor and select variants capable of detecting ligands that are structurally-related to the original ligand. The selection strategy is illustrated in Fig. 9A for a partially-randomized version of our guanine sensor. The partially-randomized pool will contain RNAs with a wide variety of sequences but each RNA will be related to the guanine sensor. The hypothesis is that some of the variants will have altered ligand specificity. The system is identical to the fluorescence quenching assay except biotin, rather than a quencher, is placed at the 5′ end of 5′T-7, and the biotinylated oligos are attached to streptavidin-coated magnetic beads. The RNAs in the initial RNA pool are labeled with fluorescein and immobilized on the beads by annealing to 5′T-7. After washing to remove unbound RNA, the beads are incubated with the desired ligand and RNAs that elute from the beads are collected. The eluted RNAs are amplified by reverse transcription-polymerase chain reaction (RT-PCR) and the resulting cDNAs are used as templates to transcribe a new RNA pool. In the early rounds of selection, most of the eluted RNA represents background due to random dissociation from 5′T-7. Subsequent rounds of selection enrich the pool for RNAs that elute efficiently only when bound to the ligand. The selection is continued until the amount of RNA that elutes from the beads reaches a maximum. Finally, cDNAs derived from the eluted RNA are sequenced to identify the selected RNAs.

We first asked whether we could anneal the guanine sensor to 5′T-7 when 5′T-7 was bound to magnetic beads, and whether the sensor would elute from the beads in the presence of guanine and 3′T-3. We

added 180 pmol of heat-denatured *xpt* RNA (1–91) to magnetic beads with 200 pmol of bound 5′T-7. We found that the annealing reaction was very slow. After incubating overnight, only about 30 pmol of RNA was bound to the beads. Longer incubation times did not result in more RNA binding. This result suggested that a large fraction of 5′T-7 on the beads was inaccessible to the RNA. We then measured the amount of RNA eluted from the beads after incubation for various lengths of time with 5 μM guanine and 150 pmol of 3′T-3 under the same conditions as used for the quenching assay. We measured the level of background elution by incubating the beads under identical conditions but in the absence of guanine. We found that the highest signal-to-background ratio was achieved with an incubation time of 6 h.

Interestingly, we found that the signal-to-background ratio increased when the experiment was performed without 3′T-3. This was due to the fact that the amount of RNA eluted with buffer (background) decreased more than the amount of RNA eluted with guanine (signal). 3′T-3 had the opposite effect on the fluorescence quenching assay (data not shown). The role of 3′T-3 is to capture 5′T-7 as it dissociates from *xpt* RNA (1–91), thus driving the strand exchange reaction in the forward direction. However, since the RNA binds very slowly when 5′T-7 is on the beads, it appeared that 3′T-3 was not required to prevent the eluted RNA from re-attaching to the beads during the 6 h incubation. Under the optimal conditions, about 7.5 pmol (25%) of the bound *xpt* RNA (1–91) eluted with 5 μM guanine. Only about 0.8 pmol (~2.5%) of RNA eluted when the beads were incubated with assay buffer only, giving a ~10:1 signal-to-background ratio.

To test our selection scheme, we performed a proof-of-principle experiment. To produce the initial RNA pool, we partially randomized the sequence of our guanine sensor and bound ~30 pmol (1.8×10^{13} molecules) of the RNA to the magnetic beads as described above. We randomized the sequences of only the joining regions (J1-2, J2-3, and J3-1) and the base pairs at the bottom of the P1, P2, and P3 stems (see Fig. 1B). We did not randomize the remainder of the stems or their single-stranded loops. Since *xpt* RNA (1–91) was only partially randomized, the initial RNA pool included a significant amount of RNA with no sequence changes. Thus, we attempted to isolate the original guanine sensor (and, possibly, functional variants) by using guanine as the ligand during selection. After only 4 rounds of selection, the RNA elution efficiency increased from background levels (~2% elution) to about 20% elution. The elution efficiency did not increase with further rounds of selection. Since 20% elution is similar to the elution efficiency of pure *xpt* RNA (1–91) (~25%), we predicted that our selected RNA pool consisted primarily of *xpt* RNA (1–91). We sequenced 16 cDNA clones prepared from the selected RNA and found that the sequences of 9 of the clones were identical to that of *xpt* RNA (1–91) (Fig. 9B). Three of the sequences differed from *xpt* RNA (1–91) at only 1 or 2 positions (clones S6, S8, and S11 in Fig. 9B). Clone S6 had two sequence changes that converted the A25-U45 pair at the base of stem P2 to a G-C pair. It is known that the structure of the P2 stem is an important determinant of ligand affinity and specificity (Edwards and Batey, 2009). Clone S8 had a single base change that disrupted the G27-C43 pair near the middle of P2 by changing the G27 pair to a U. Since this base was not changed in the original randomized RNA pool, it probably arose during the selection due to an error made by reverse transcriptase or Taq DNA polymerase. Clone S11 changed U48 in J2-3 to a C. It is known that U48 bulges out of the ligand binding pocket and does not contact the bound guanine (Serganov et al., 2004), so it is not surprising that *xpt* RNA (1–91) could tolerate this change. The other 4 sequences (clones S3, S9, S16, and S17) contained a large number of changes compared to *xpt* RNA (1–91) and probably represented RNAs that eluted randomly from the beads (not shown in Fig. 9B). We transcribed the RNAs encoded by clones S6, S8, and S11 and S3, and tested each of them for their ability to detect 100 nM guanine in the fluorescence quenching assay (Fig. 9C). The fluorescence signals produced by both S6 and S8 RNA were about half that produced by *xpt* RNA (1–91). These results are consistent with the known effects of mutations in the P2 stem of the guanine riboswitch (Edwards and Batey, 2009). S11 RNA gave the same signal as *xpt* RNA (1–91). S3, the RNA with a highly divergent sequence could not detect 100 nM guanine.

4. Discussion

Although much work has focused on using riboswitches as biosensors *in vivo*, less effort has been exerted toward using riboswitches to detect ligands *in vitro*. One highly successful approach for making sensors for both *in vitro* and *in vivo* detection of ligands has been to fuse various aptamer domains *via* a short “communication module” to a fluorescent aptamer such as “Spinach” (Litke et al., 2016; Paige et al., 2011; Nakayama et al., 2012; Kellenberger et al., 2013; Bhadra and Ellington, 2014; Kellenberger et al., 2015; Ketterer et al., 2016; Bose et al., 2016). The fusions are designed such that ligand binding to the aptamer domain allows the fluorescent aptamer to fold into its active conformation. However, this approach often requires fairly extensive re-design and optimization for each new aptamer domain. Our work sought to convert riboswitches into highly sensitive and specific sensors and to devise a system that would facilitate the isolation of sensors with novel ligand specificities without the need for extensive optimization for each new sensor. This was accomplished by exploiting the modular nature of riboswitches and optimizing the stabilities of the ligand-free and ligand-bound forms of our sensors. We are currently testing whether this approach can be extended to aptamer domains from riboswitches that detect ligands other than purine derivatives and riboswitches that activate rather than inhibit gene expression upon ligand binding. As shown by Ceres et al. designing hybrid “ON” switches poses a particular challenge (Ceres et al., 2013bb).

We realized that our approach would not necessarily work for every riboswitch and, of course, nature has not designed riboswitches that can detect every possible ligand of interest. Many groups have attempted to extend the ligand specificity of sensors by replacing naturally-occurring aptamer domains with RNA aptamers produced by *in vitro* selection using the standard SELEX protocol. This approach has been successful for some applications but has also failed because ligand binding did not induce the required conformational change (Robertson and Ellington, 2000). To circumvent this problem, we and others previously devised an *in vitro* selection strategy for isolating RNAs that not only bind to the desired ligand but that are also guaranteed to undergo a desired conformational change (Nutiu and Li, 2005; Morse, 2007; Rajendran and Ellington, 2008; Vandenengel and Morse, 2009). Based on our sensor design and our previous selection strategy, we devised a scheme for changing the ligand specificity of naturally-occurring riboswitches.

For our proof-of-principle selection experiment, we partially randomized the ligand-binding domain of the guanine riboswitch and attempted to isolate the original guanine riboswitch using guanine as the ligand. The success of this experiment showed that our strategy works. In addition to isolating the original guanine riboswitch, we found three functional variants, indicating that our selection scheme will also be useful for structure-function studies. We sequenced only 16 of the RNAs selected with guanine, but deep sequencing should reveal most, if not all, of the possible functional variants.

Importantly, each of our hybrid sensors represent a new starting point for *in vitro* selection and there will be no need to extensively optimize the conditions for each new selection. Thus, we should be able to find sensors for ligands related to the cognate ligand of each riboswitch, and we will be able to perform studies that probe the sequence and structure requirements for each new ligand-binding domain.

It is instructive to compare our selection scheme to recently reported experiments. Koizumi et al. completely randomized the aptamer domain of a self-cleaving allosteric hammerhead ribozyme and selected novel aptazymes that could detect cGMP, cAMP, and cCMP (Koizumi et al., 1999). Schemes for selecting functional self-cleaving ribozymes have an intrinsic advantage over selecting riboswitches. Functional

ribozymes can be cleanly separated from non-functional variants by isolating cleavage fragments. (Koizumi et al. used electrophoresis to do this.) Thus, there is very little background to overcome during the selection. In our strategy for selecting riboswitches, we collect RNAs that dissociate from immobilized 5′T-7 upon ligand binding, but about 2% of this RNA dissociates randomly, independent of ligand binding. Thus, we see no increase in the amount of eluted RNA until functional RNAs comprise greater than 2% of the selected population. With this relatively high background, it is more likely that rare functional variants will be lost if many rounds of selection are required to purify the desired RNAs. However, deep sequencing of the selected RNAs should obviate this problem since functional variants could be identified as having been enriched after only a few rounds of selection. Additionally, we could reduce (but not eliminate) background by reversing our strategy and capturing functional RNAs through annealing the RNA to immobilized 3′T-3. In this strategy, 5′T-7 would be covalently linked to the aptamer domain of a riboswitch through an RNA linker. A similar approach was reported recently for the selection of TPP sensors (Martini et al., 2015). Another source of our relatively high background is that a significant fraction of the immobilized 5′T-7 is inaccessible or sterically hindered resulting in very slow annealing of RNAs. Thus, elution of RNAs from the beads is essentially irreversible during our 6 h elution reaction. A possible solution to this problem is to use a longer linker between 5′T-7 and biotin on its 5′ end or reduce the density of 5′T-7 on the beads. Randomly eluted RNAs should more readily re-anneal to the more accessible 5′T-7, while ligand-bound RNAs should re-anneal slowly. This approach may result in the need to include 3′T-3 in the selection to further decrease the rate at which functional RNAs re-anneal to 5′T-7.

In another recent paper, Porter et al. used the standard SELEX procedure to find variants of the aptamer domain of the *xpt*-guanine riboswitch that could bind to 5-hydroxytryptophan and 3,4-dihydroxyphenylalanine (Porter et al., 2017). The selected variants were converted into robust sensors for their ligands by fusing them to a Broccoli aptamer *via* a communication module. Our selection strategy inverts the standard SELEX procedure. Rather than selecting RNAs that bind to an immobilized ligand, we anneal the randomized RNA pool *via* base-pairing to an immobilized oligo and select RNAs that elute upon binding to the ligand. The selected RNAs can then be directly used as *in vitro* sensors *via* our quenching assay. Thus, the additional step of fusing the selected RNAs to a fluorescent aptamer will not be required.

We are interested in finding variants of our guanine sensor that can detect hypoxanthine but not guanine. Hypoxanthine is identical to guanine except for the absence of the extracyclic amino group found in guanine. A hypoxanthine sensor that cannot bind to guanine would have to prevent guanine binding through a steric clash with the extra amino group, but still make productive contacts with other regions of the base. This would be a challenge to achieve through rational design as it would likely require multiple base changes.

5. Conclusion

Riboswitches are being applied as analytical tools in biochemistry, genetics, cell biology, medicine, environmental science, forensics, and many other areas (Lee et al., 2016; Machtel et al., 2016). In the exciting new field of synthetic biology, riboswitches have become the preferred tool for constructing new gene regulatory devises and genetic circuits (Groher and Suess, 2014; Jo and Shin, 2009; Topp et al., 2010; Weber and Fussenegger, 2011; Chappell et al., 2015). Our work will contribute to increasing the availability of riboswitches with novel ligand specificity.

Funding

This work was supported by the Defense Threat Reduction Agency [MIPR HDTRA1620511 to D.M.]; the Office of Naval Research; and the Chemistry Department of the U.S. Naval Academy.

Acknowledgements

Thanks to Shirley Lin and Ina O'Carroll for critical reading of the manuscript.

References

Serganov, A., Nudler, E., 2013. A decade of riboswitches. Cell 152, 17–24.
Fowler, C.C., Brown, E.D., Li, Y., 2010. Using a riboswitch sensor to examine coenzyme B (12) metabolism and transport in E. coli. Chem Biol. 17, 756–765.
Fowler, C.C., Sugiman-Marangos, S., Junop, M.S., Brown, E.D., Li, Y., 2013. Exploring intermolecular interactions of a substrate binding protein using a riboswitch-based sensor. Chem. Biol. 20, 1502–1512.
You, M., Litke, J.L., Jaffrey, S.R., 2015. Imaging metabolite dynamics in living cells using a Spinach-based riboswitch. Proc. Natl. Acad. Sci. U. S. A. 112, E2756–2765.
Su, Y., Hickey, S.F., Keyser, S.G., Hammond, M.C., 2016. In vitro and in vivo enzyme activity screening via RNA-based fluorescent biosensors for S-adenosyl-l-homocysteine (SAH). J. Am. Chem. Soc. 138, 7040–7047.
Topp, S., Gallivan, J.P., 2010. Emerging applications of riboswitches in chemical biology. ACS Chem. Biol. 5, 139–148.
Chappell, J., Takahashi, M.K., Meyer, S., Loughrey, D., Watters, K.E., Lucks, J., 2013. The centrality of RNA for engineering gene expression. Biotechnol. J. 8, 1379–1395.
Groher, F., Suess, B., 2014. Synthetic riboswitches—a tool comes of age. Biochim. Biophys. Acta 1839, 964–973.
Etzel, M., Morl, M., 2017. Synthetic riboswitches: from plug and pray toward plug and play. Biochemistry 56, 1181–1198.
Hallberg, Z.F., Su, Y., Kitto, R.Z., Hammond, M.C., 2017. Engineering and in vivo applications of riboswitches. Ann. Rev. Biochem. 86, 515–539.
Ceres, P., Garst, A.D., Marcano-Velazquez, J.G., Batey, R.T., 2013a. Modularity of select riboswitch expression platforms enables facile engineering of novel genetic regulatory devices. ACS Synth. Biol. 2, 463–472.
Ceres, P., Trausch, J.J., Batey, R.T., 2013b. Engineering modular 'ON' RNA switches using biological components. Nucleic Acids Res. 41, 10449–10461.
Litke, J.L., You, M., Jaffrey, S.R., 2016. Developing fluorogenic riboswitches for imaging metabolite concentration dynamics in bacterial cells. Methods Enzymol. 572, 315–333.
Rossmanith, J., Narberhaus, F., 2016. Exploring the modular nature of riboswitches and RNA thermometers. Nucleic Acids Res. 44, 5410–5423.
Soukup, G.A., Breaker, R.R., 1999. Design of allosteric hammerhead ribozymes activated by ligand-induced structure stabilization. Structure 7, 783–791.
Robertson, M.P., Ellington, A.D., 2000. Design and optimization of effector-activated ribozyme ligases. Nucleic Acids Res. 28, 1751–1759.
Sharma, V., Nomura, Y., Yokobayashi, Y., 2008. Engineering complex riboswitch regulation by dual genetic selection. J. Am. Chem. Soc. 130, 16310–16315.
Serganov, A., Yuan, Y.R., Pikovskaya, O., Polonskaia, A., Malinina, L., Phan, A.T., Hobartner, C., Micura, R., Breaker, R.R., Patel, D.J., 2004. Structural basis for discriminative regulation of gene expression by adenine- and guanine-sensing mRNAs. Chem. Biol. 11, 1729–1741.
Gilbert, S.D., Stoddard, C.D., Wise, S.J., Batey, R.T., 2006. Thermodynamic and kinetic characterization of ligand binding to the purine riboswitch aptamer domain. J. Mol. Biol. 359, 754–768.
Edwards, A.L., Batey, R.T., 2009. A structural basis for the recognition of 2'-deoxyguanosine by the purine riboswitch. J. Mol. Biol. 385, 938–948.
Nutiu, R., Li, Y., 2005. In vitro selection of structure-switching signaling aptamers. Angew. Chem. Int. Ed. Engl. 44, 1061–1065.
Morse, D.P., 2007. Direct selection of RNA beacon aptamers. Biochem. Biophys. Res. Commun. 359, 94–101.
Rajendran, M., Ellington, A.D., 2008. Selection of fluorescent aptamer beacons that light up in the presence of zinc. Anal. Bioanal. Chem. 390, 1067–1075.
Vandenengel, J.E., Morse, D.P., 2009. Mutational analysis of a signaling aptamer suggests a mechanism for ligand-triggered structure-switching. Biochem. Biophys. Res. Commun. 378, 51–56.
Mandal, M., Boese, B., Barrick, J.E., Winkler, W.C., Breaker, R.R., 2003. Riboswitches control fundamental biochemical pathways in Bacillus subtilis and other bacteria. Cell 113, 577–586.
Kim, J.N., Roth, A., Breaker, R.R., 2007. Guanine riboswitch variants from Mesoplasma florum selectively recognize 2'-deoxyguanosine. Proc. Natl. Acad. Sci. U. S. A. 104, 16092–16097.
Sudarsan, N., Lee, E.R., Weinberg, Z., Moy, R.H., Kim, J.N., Link, K.H., Breaker, R.R., 2008. Riboswitches in eubacteria sense the second messenger cyclic di-GMP. Science 321, 411–413.
Steinert, H., Sochor, F., Wacker, A., Buck, J., Helmling, C., Hiller, F., Keyhani, S., Noeske, J., Grimm, S., Rudolph, M.M., et al., 2017. Pausing guides RNA folding to populate transiently stable RNA structures for riboswitch-based transcription regulation. Elife 6.
Gilbert, S.D., Reyes, F.E., Edwards, A.L., Batey, R.T., 2009. Adaptive ligand binding by the purine riboswitch in the recognition of guanine and adenine analogs. Structure 17, 857–868.
Paige, J.S., Wu, K.Y., Jaffrey, S.R., 2011. RNA mimics of green fluorescent protein. Science 333, 642–646.
Nakayama, S., Luo, Y., Zhou, J., Dayie, T.K., Sintim, H.O., 2012. Nanomolar fluorescent

detection of c-di-GMP using a modular aptamer strategy. Chem. Commun. (Camb.) 48, 9059–9061.
Kellenberger, C.A., Wilson, S.C., Sales-Lee, J., Hammond, M.C., 2013. RNA-based fluorescent biosensors for live cell imaging of second messengers cyclic di-GMP and cyclic AMP-GMP. J. Am. Chem. Soc. 135, 4906–4909.
Bhadra, S., Ellington, A.D., 2014. A spinach molecular beacon triggered by strand displacement. RNA 20, 1183–1194.
Kellenberger, C.A., Chen, C., Whiteley, A.T., Portnoy, D.A., Hammond, M.C., 2015. RNA-based fluorescent biosensors for live cell imaging of second messenger cyclic di-AMP. J. Am. Chem. Soc. 137, 6432–6435.
Ketterer, S., Gladis, L., Kozica, A., Meier, M., 2016. Engineering and characterization of fluorogenic glycine riboswitches. Nucleic Acids Res. 44, 5983–5992.
Bose, D., Su, Y., Marcus, A., Raulet, D.H., Hammond, M.C., 2016. An RNA-based fluorescent biosensor for high-throughput analysis of the cGAS-cGAMP-STING pathway. Cell Chem. Biol. 23, 1539–1549.
Koizumi, M., Soukup, G.A., Kerr, J.N., Breaker, R.R., 1999. Allosteric selection of ribozymes that respond to the second messengers cGMP and cAMP. Nat. Struct. Biol. 6, 1062–1071.
Martini, L., Meyer, A.J., Ellefson, J.W., Milligan, J.N., Forlin, M., Ellington, A.D., Mansy, S.S., 2015. In vitro selection for small-molecule-triggered strand displacement and riboswitch activity. ACS Synth. Biol. 4, 1144–1150.
Porter, E.B., Polaski, J.T., Morck, M.M., Batey, R.T., 2017. Recurrent RNA motifs as scaffolds for genetically encodable small-molecule biosensors. Nat. Chem. Biol. 13, 295–301.
Lee, C.H., Han, S.R., Lee, S.W., 2016. Therapeutic applications of aptamer-based riboswitches. Nucleic Acid Ther. 26, 44–51.
Machtel, P., Bakowska-Zywicka, K., Zywicki, M., 2016. Emerging applications of riboswitches - from antibacterial targets to molecular tools. J. Appl. Genet. 57, 531–541.
Jo, J.J., Shin, J.S., 2009. Construction of intragenic synthetic riboswitches for detection of a small molecule. Biotechnol. Lett. 31, 1577–1581.
Topp, S., Reynoso, C.M., Seeliger, J.C., Goldlust, I.S., Desai, S.K., Murat, D., Shen, A., Puri, A.W., Komeili, A., Bertozzi, C.R., et al., 2010. Synthetic riboswitches that induce gene expression in diverse bacterial species. Appl. Environ. Microbiol. 76, 7881–7884.
Weber, W., Fussenegger, M., 2011. Emerging biomedical applications of synthetic biology. Nat. Rev. Genet. 13, 21–35.
Chappell, J., Watters, K.E., Takahashi, M.K., Lucks, J.B., 2015. A renaissance in RNA synthetic biology: new mechanisms, applications and tools for the future. Curr. Opin. Chem. Biol. 28, 47–56.